MOLECULAR IMAGING AND BIOLOGY

Mol Imaging Biol (2019) 21:722–730
DOI: 10.1007/s11307-018-1268-x

Published Online: 17 September 2018

RESEARCH ARTICLE

Adenine Nucleotide Translocase 2 as an Enzyme Related to [^{18}F] FDG Accumulation in Various Cancers

Chul-Hee Lee,[1,2,3,4] Mi Jeong Kim,[1,3,4] Hwan Hee Lee,[1] Jin Chul Paeng,[1] Young Joo Park,[5] So Won Oh,[1,6] Young Jun Chai,[7] Young A. Kim,[8] Gi Jeong Cheon,[1,3] Keon Wook Kang,[1,3] Hyewon Youn,[1,3,4,9] June-Key Chung[1,2,3,4]

[1]*Department of Nuclear Medicine, Seoul National University College of Medicine, Seoul, South Korea*
[2]*Biomedical Sciences, Seoul National University College of Medicine, Seoul, South Korea*
[3]*Cancer Research Institute, Seoul National University College of Medicine, Seoul, South Korea*
[4]*Tumor Microenvironment Global Core Research Center, Seoul National University, Seoul, South Korea*
[5]*Department of Internal Medicine, Seoul National University College of Medicine, Seoul, South Korea*
[6]*Department of Nuclear medicine, Seoul National University Boramae Medical Center, Seoul, South Korea*
[7]*Department of Surgery, Seoul National University Boramae Medical Center, Seoul, South Korea*
[8]*Department of Pathology, Seoul National University Boramae Medical Center, Seoul, South Korea*
[9]*Cancer Imaging Center, Seoul National University Hospital, Seoul, South Korea*

Abstract

Purpose: Although glucose transporter 1 (GLUT1) and hexokinase 2 (HK2) are known as major proteins involved in the molecular mechanisms for accumulating 2-deoxy-2-[^{18}F]fluoro-D-glucose ([^{18}F]FDG) in cancer cells, sometimes, [^{18}F] FDG accumulation cannot be explained by the expression of these two proteins. We investigated the involvement of adenine nucleotide translocase 2 (ANT2), which catalyzes ADP/ATP exchange at the mitochondrial inner membrane, in [^{18}F] FDG accumulation.

Procedures: ANT2 expression was evaluated in various cancer cell lines and human cancer tissues (microarrays) using western blot and immunohistochemical (IHC) staining, respectively. The expression levels of ANT2 were compared to [^{18}F] FDG accumulation and pathologic findings, including differentiation grade. Additionally, we modulated ANT2 expression levels using *ANT2* siRNA and an *ANT2* expression vector in cancer cells and murine xenografted tumors.

Results: [^{18}F] FDG accumulation correlated with ANT2 expression in various cancer cell lines; this was not explained by GLUT1 and/or HK2 expression. At both the cell and tissue levels, ANT2 expression was high in less-differentiated or more malignant type of cancers. [^{18}F] FDG accumulation changed according to the modulation of the ANT2 expression level.

Conclusion: In various cancer cells and tissues, the expression levels of ANT2 explained [^{18}F] FDG accumulation better than those of GLUT1 and HK2. ANT2 can be used as a marker of dedifferentiated pathology and aggressiveness of cancer.

Electronic supplementary material The online version of this article (https://doi.org/10.1007/s11307-018-1268-x) contains supplementary material, which is available to authorized users.

Correspondence to: Hyewon Youn; *e-mail:* hwyoun@snu.ac.kr, June-Key Chung; *e-mail:* jkchung@snu.ac.kr

Key words: [18F]FDG-PET, GLUT1, HK2, Adenine nucleotide translocase 2 (ANT2), Differentiation of cancer

Introduction

Most cancer cells depend on inefficient glycolysis for ATP production. Therefore, cancer cells use huge amounts of glucose to maximize ATP production [1, 2]. 2-Deoxy-2-[18F]fluoro-D-glucose ([18F]FDG), a glucose analogue, was developed to visualize cancer cells using positron emission tomography (PET) [3]. Currently, [18F]FDG-PET is one of the essential imaging modalities in the management of cancer patients [4–6]. Although the main indications of clinical [18F]FDG-PET are staging and detection of recurrence, assessment of tumor malignancy is another indication. Several investigators have reported the correlation of [18F] FDG accumulation with tumor grade, stage, and prognosis in many cancers including non-small cell lung cancer (NSCLC) [7–9].

Two major proteins are involved in uptake of [18F] FDG in normal and cancer cells. [18F] FDG is transported into cells by glucose transporters (GLUTs) and phosphorylated by the hexokinases (HKs) to form [18F]FDG-6-phosphate ([18F]FDG-6-P) [10, 11]. Unlike glucose, [18F]FDG-6-P cannot be further phosphorylated and is trapped within cells. F-18-labeled [18F] FDG provides an image of glucose metabolism [12]. Cancer cells generally express elevated levels of GLUTs [13] and HKs [14], especially GLUT1 and HK2 [15, 16], which induce high [18F] FDG accumulation in cancer cells [12, 17, 18]. However, sometimes, high [18F] FDG accumulation cannot be explained by the expression of these two proteins [19–21].

Recently, HK2 has been suggested to be more important in [18F] FDG accumulation than GLUT1 [15]. HK2 is physically associated with mitochondrial outer-membrane proteins (porin or the voltage-dependent anion channel, VDAC) for the preferential use of ATP derived from the mitochondria [22, 23]. The role of VDAC in the activity of the HKs has been widely studied [24, 25]. A large amount of mitochondria-bound HK2 induces high anaerobic glycolysis rates in cancer cells [26].

Adenine nucleotide translocases (ANTs) are mainly involved in cellular energy metabolism by catalyzing the ADP/ATP exchange across the mitochondrial inner membrane [27]. During glucose phosphorylation, ANTs can bind to VDAC, supplying ATP to mitochondrial HK2 [26]. The expression of one ANT, ANT2, is inducible in proliferative cells and has been associated with cancer malignancy [28, 29]. Additionally, another study demonstrated that ANT2 expression converts cell metabolism processes to glycolysis in cancer cells [30]. However, the expression of ANT2 with regard to [18F] FDG metabolism has not yet been investigated. Especially, the relationship between [18F] FDG accumulation and the protein level of ANT2, when compared with GLUT1 and HK2 levels, is not yet clear.

In this study, we measured ANT2 expression in various cancer cell lines and human cancer tissues using western blotting and immunohistochemical (IHC) staining, respectively. The expression level of ANT2 was compared to [18F] FDG accumulation and pathologic findings, including the differentiation grade. Additionally, we modulated ANT2 expression using *ANT2* siRNA and an *ANT2* expression vector in cancer cells and xenografted tumors and monitored the changes of [18F] FDG uptake.

Materials and Methods

Cell Lines

Normal human thyroid (Nthy-ori) and thyroid cancer (WRO, B-CPAP, BHP10-3, TPC-1, and FRO), breast cancer (MCF-7, MDA-MB231), prostate cancer (DU145, PC3), hepatoma (Hep3B, SK-Hep1), glioma (U87MG, U373), and lung cancer (H358, A549, H520, H460) cell lines were used. Cells were incubated in a humidified incubator at 37 °C with a 5 % CO_2 atmosphere.

Western Blot Analysis

Protein concentrations were determined with BCA protein assay kit (Thermo Scientific). The membranes were blocked for 1 h at room temperature and incubated with one of the following primary antibodies overnight at 4 °C: anti-GLUT1 (#ab652, Abcam; diluted 1:1000), or anti-HK2 (#2867, Cell signaling Technology; diluted 1:1000), or anti-ANT2 (#12546, Cell signaling Technology; diluted 1:1000), or β-actin (#A5441, Sigma-Aldrich). An enhanced chemical luminescence reagent (Roche) was used; luminescent signals were measured with an LAS-3000 imaging system (Fujifilm).

In vitro [18F] FDG Uptake Assay

Cells were pre-incubated with glucose-free medium for 4 h and trypsinized. Uptake was examined using 0.185 MBq/ml of [18F] FDG in assay medium (HBSS, 0.5 % bovine serum albumin [*w*/*v*], pH 7.4). Incubation was performed for 1 h at 37 °C. The cells were washed thrice with cold HBSS and lysed with 1 % sodium dodecyl sulfate (SDS). Radioactivity of the cell lysates was measured using a Cobra II gamma counter (Canberra Packard). Radioactivity

was normalized with the amount of total protein at the time of the assay. All experiments were performed at least in triplicate. Results were analyzed according to the pathological types of cancer cells.

Tissue Microarrays

Tissue microarrays (TMAs) from patients who were diagnosed with less-differentiated thyroid cancer were kindly provided by Dr. Park YJ (Department of Internal Medicine, Seoul National University Hospital, Seoul, Korea). The study has been approved by the Institutional Review Board and all subjects signed an informed consent form. TMAs were reviewed at the Department of Pathology, Seoul National University, and Seoul National University Boramae Medical Center.

We also purchased commercially available TMAs of NSCLC and hepatocellular carcinoma (Superbiochips Laboratories, Seoul, Korea) to expand the tissue analysis. Tissue cores from these tumors were also classified according to their pathologic findings.

Immunohistochemistry of TMAs

Core tissue biopsies (2 mm in diameter) were arranged in a new recipient paraffin block to generate TMAs using a trephine apparatus (Superbiochips Laboratories). The antigen was retrieved and the samples were then treated with the primary antibodies overnight at 4 °C and then with the biotinylated secondary antibodies. The primary or secondary antibodies were used as follows: anti-ANT2 (#17796-1-AP, Proteintech; diluted 1:300); biotinylated anti-rabbit for ANT2 (Dako; diluted 1:500). Avidin-biotin peroxidase complexes were used for amplification and developed by using 3,3′-diaminobenzidine (DAB). Scoring was evaluated by three independent investigators and performed according to a five-grade scale: 1, no staining signal; 2, weak signal or a few cells stained; 3, medium signal; 4, strong signal localized in a certain area; 5, strong staining of the whole area [31].

Construction of the ANT2 Expression Vector and ANT2 siRNA

The *ANT2* expression vector (pcDNA3.1-ANT2) was kindly provided by Dr. Kim CW (Seoul National University, Seoul, South Korea). Antisense-*ANT2* siRNA and scramble were synthesized by ST Pharm Co. For protection against nucleases, the siRNAs contained 2-methoxy (2-OMe) cytosine and uracil [32].

Transfection for the Upregulation or Downregulation of ANT2

Cells were plated in 6-well plates with antibiotic-free medium, and transfected with Lipofectamine 2000 (Invitrogen), according to the manufacturer's instructions. Cells were harvested 48 h after transfection. Western blots were performed to validate the upregulation or downregulation of ANT2 expression.

Animal Experiments

Six-week-old male BALB/c nude mice were obtained from Orient Bio, Inc. All experiments were approved by the Institutional Animal Care and Use Committee of the Seoul National University Hospital (SNUH-IACUC). For establishment of tumor xenograft mouse models ($n = 6$ for each group), luciferase-expressing FRO cells (2×10^6) were transplanted subcutaneously into both thighs. Intra-tumoral injections of 10 nM scramble siRNA or *ANT2* siRNA supplemented with lipofectamine 2000 were administered from 2 weeks after tumor inoculation, when the tumor sizes were < 0.5 cm in diameter. Bioluminescence imaging (BLI) and small-animal PET imaging were performed before and after the injections.

In vivo Bioluminescence Imaging

The IVIS 100 imaging system (Caliper Life Sciences) was used to obtain bioluminescent images and to quantify optical signals. D-luciferin potassium salt (0.3 mg/ml in PBS) was intraperitoneally injected into mice. After 10 min, optical signals were obtained and quantified by drawing regions of interest (ROIs) on the tumors. Signal intensity was presented as photons/cm2/second/steradian (p/cm2/s/sr).

Animal PET Imaging

PET images of tumor-bearing mice were acquired using PET box (SOFIE Bioscience). Mice were fasted for at least 6 h and injected with 1.11–1.48 MBq of [18F] FDG *via* the tail vein. PET images were obtained 60 min after the injection. Static scans (for 2-min scan) were obtained, and the images were reconstructed with AMIDE algorithm (A Medical Image Data Examiner). A semi-automated ROI was generated around the area of each tumor in three dimensions by drawing an isocontour with a threshold, which is equal to the calculated average background uptake of the mouse. Maximum [18F] FDG uptake was calculated to measure [18F] FDG uptake within this ROI.

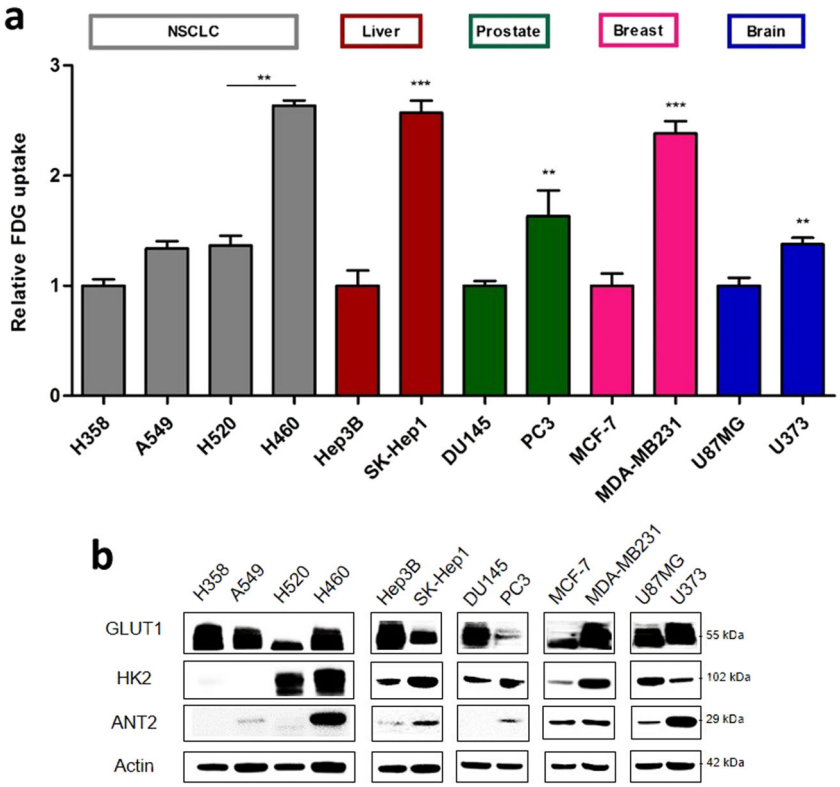

Fig. 1. Comparison between the [18F] FDG uptake and expression levels of GLUT1, HK2, and ANT2 in various cancer cell lines. **a** Relative [18F] FDG accumulation in various cancer cell lines, NSCLC (H358, A549, H520, and H460), liver (Hep3B, SK-Hep1), prostate (DU145, PC3), breast (MCF-7, MDA-MB231), and brain (U87MG, U373). Cancer cells show different patterns of [18F] FDG uptake according to their pathologic types. **b** Protein levels of GLUT1, HK2, and ANT2 measured by western blot.

IHC of the Grafted Tumor

The primary antibodies used were as follows: anti-GLUT1 (#ab652, Abcam; diluted 1:1000), anti-HK2 (GTX111525, GeneTex; diluted 1:1500), and anti-ANT2 (same as above). The secondary antibodies used were as follows: biotinylated anti-rabbit for GLUT1, HK2, and ANT2 (Dako; diluted 1:500). The samples were amplified with avidin-biotin peroxidase complexes and developed using DAB. Then, the samples were slightly counterstained with hematoxylin.

Statistical Analysis

All statistical analyses were performed using the GraphPad prism software. All data are expressed as means ± standard deviation (SD) and are representative of at least two separate biological experiments performed in triplicate. Statistical significance between the groups was compared using one-way ANOVA and unpaired Student's t test. $P < 0.05$ was considered statistically significant.

Results

Relationship Between [18F] FDG Accumulation and ANT2 Expression in Various Cancer Cells

The [18F] FDG uptake in various cancer cell lines differed significantly (Fig. 1a). Among NSCLC cells, [18F] FDG accumulation was higher in H460 cells than in the other cancer cell lines ($P < 0.001$); high levels of GLUT1 and HK2 expression were also observed. Likewise, ANT2 expression was much higher in H460 cells than in the other cells (Fig. 1b). [18F] FDG uptake was significantly higher in SK-Hep1 ($P < 0.001$), PC3 ($P < 0.01$), MDA-MB-231 ($P < 0.001$), and U373 ($P < 0.01$) cells than in other cells among the same cancer cell types (Fig. 1a). When comparing the [18F] FDG uptake with GLUT1 and HK2 levels, except for the case of the breast cancer cell lines, the different expression of both proteins was insufficient to explain the [18F] FDG accumulation. On the other hand, ANT2 expression was significantly high in all the cell types, especially in U373 cells, with high [18F] FDG accumulation (Fig. 1b).

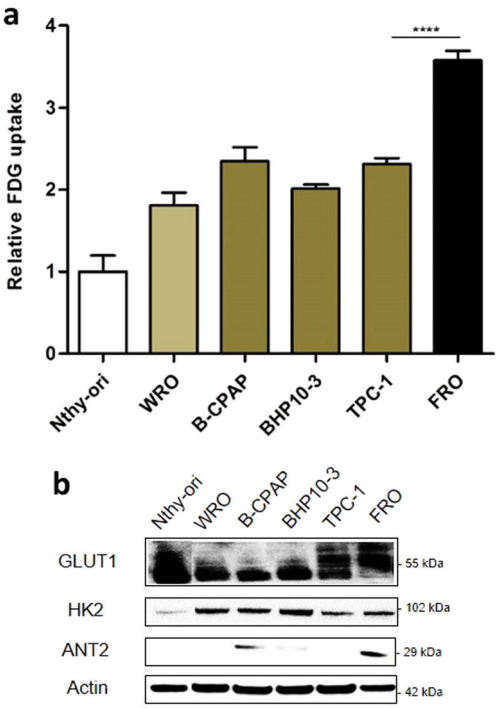

Fig. 2. Comparison between [18F] FDG uptake and expression level of GLUT1, HK2, and ANT2 in thyroid cancer cells. **a** Relative [18F] FDG accumulation in thyroid cell lines, normal (Nthy-ori), follicular carcinoma (WRO), papillary carcinoma (B-CPAP, BHP10-3, and TPC-1), and anaplastic carcinoma (FRO). **b** Protein levels of GLUT1, HK2, and ANT2 measured by western blot.

[18F] FDG Accumulation and ANT2 Expression in Thyroid Cancer Cell Lines

The [18F] FDG uptake in different thyroid cancer cells was clearly higher than that of normal thyroid cells (Nthy-ori). Among the thyroid cancer cell lines, anaplastic thyroid cancer FRO cells had the highest [18F] FDG uptake ($P < 0.001$) (Fig. 2a). GLUT1 expression was elevated to varying degrees in all the thyroid cell lines (*i.e.*, normal and cancer cells). In contrast, HK2 expression was high in the cancer cells. Anaplastic FRO cells showed the highest ANT2 expression (Fig. 2b). Although both FRO and TPC-1 cells had strong GLUT1 and HK2 expressions, ANT2 expression was only observed in the FRO cells.

Table 1. IHC scores for ANT2 expression in NSCLC tissue microarrays

	n	ANT2 (score)
Histology		
Normal	9	1.11 ± 0.24
Bronchioloalveolar	10	1.37 ± 0.46
Adenocarcinoma	15	1.78 ± 1.04
Squamous cell	49	2.05 ± 0.94
Large cell	8	2.83 ± 1.21
Differentiation		
Well	16	2.10 ± 1.00
Moderate	19	2.16 ± 1.06
Poor	8	3.08 ± 1.05

Table 2. IHC scores for ANT2 expression in hepatocellular carcinoma tissue microarrays

	n	ANT2 (score)
Well	6	1.78 ± 0.86
Moderate	32	2.55 ± 1.13
Poor	9	3.63 ± 1.27

Pathologic Findings and ANT2 Expression in Various Cancer Tissues

We evaluated ANT2 expression in tissue array samples including NSCLC (Table 1), hepatocellular carcinoma (Table 2), and thyroid cancer (Table 3). Poorly differentiated NSCLC had higher ANT2 expression than moderately differentiated cancer ($P < 0.05$) (Fig. 3a). ANT2 expression was higher in NSCLC tissues than in normal tissues, and showed a significant difference according to the histological subtypes ($P < 0.001$) (Fig. 3b). Furthermore, we found that ANT2 expression was elevated in the poorly differentiated type of HCC ($P < 0.01$) (Fig. 4a). Among the thyroid cancer tissues, ANT2 expression increased in PDTC and ATC tissues ($P < 0.01$) (Fig. 4b).

Changes in [18F] FDG Accumulation by Modulation of ANT2 Expression

Two thyroid cancer cells, TPC-1 and FRO, were selected for these experiments because they expressed different levels of ANT2 but similar levels of GLUT1 and HK2 (Fig. 2b). ANT2-specific upregulation (Fig. 5a) increased [18F] FDG accumulation by 1.7-fold, when compared to the control ($P < 0.05$) (Fig. 5b). ANT2-specific downregulation (Fig. 5c) decreased [18F] FDG accumulation by 0.55-fold, when compared to the control ($P < 0.0001$) (Fig. 5d).

We established mouse xenograft models and monitored the effect of si*ANT2* on [18F]FDG-PET signals. The si*ANT2* treatment significantly reduced [18F] FDG uptake compared to the scrambled control ($P < 0.05$) (Fig. 6a), even though there was no difference in the bioluminescence signals, which represented the number of viable cancer cells (Supplemental Fig. 1) (*i.e.*, control and si*ANT2*-treated). ANT2 downregulation was confirmed by the IHC of the

Table 3. IHC scores for ANT2 expression in PDTC and ATC tissue microarrays

	n	ANT2 (score)
Normal	36	1.62 ± 0.48
PDTC	44	2.08 ± 0.98
ATC	15	2.40 ± 1.28

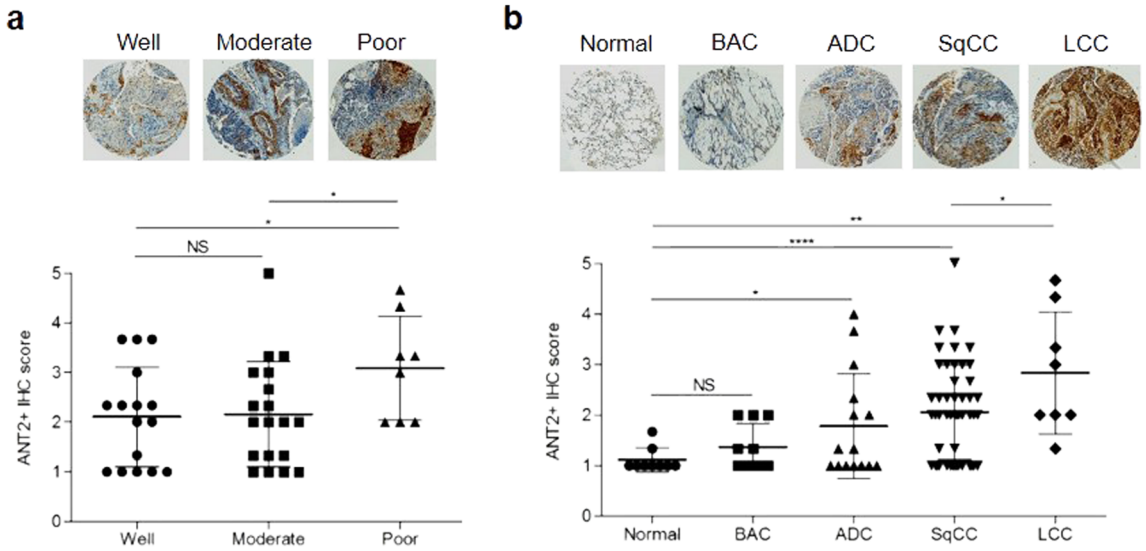

Fig. 3. Expression levels of ANT2 in NSCLC tissues measured by IHC, according to pathologic findings. **a** ANT2 expression in NSCLC based on differentiation subtypes and **b** histological subtypes. BAC, bronchioloalveolar carcinoma; ADC, adenocarcinoma; SqCC, squamous cell carcinoma; LCC, large cell carcinoma.

tumor tissues. On the other hand, GLUT1 and HK2 expressions were unchanged (Fig. 6b).

Discussion

In this study, ANT2 expression was associated with [^{18}F] FDG accumulation in cancer cells, murine xenografted tumors, and human cancer tissues. We demonstrated that ANT2 expression was more closely related to [^{18}F] FDG accumulation than GLUT1 and HK2 expression. ANT2 was also associated with pathologic differentiation status and malignant types. Additionally, we modulated ANT2 expression levels using *ANT2* siRNA and *ANT2* expression vector and found that [^{18}F] FDG accumulation changed according to the ANT2 expression level.

[^{18}F]FDG-PET has been clinically used in the management of cancer patients, such as for staging, restaging, and detection of recurrence. The differing accumulation of [^{18}F] FDG in various cancers is due to different rates of glucose metabolism. Both GLUT1 and HK2 are essential factors for

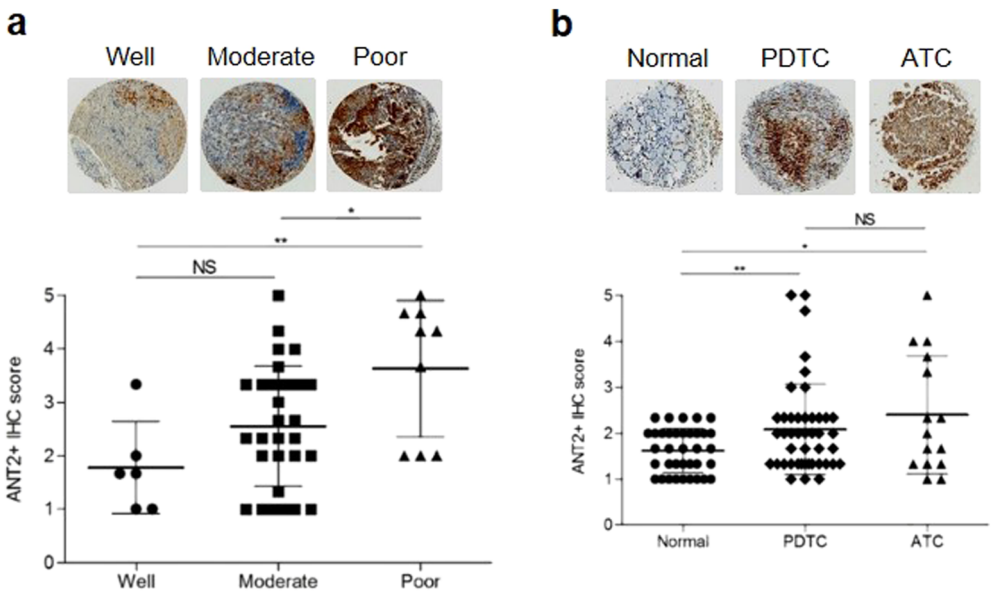

Fig. 4. Comparison between the differentiation patterns and expression levels of ANT2 in liver and thyroid cancer tissues measured by IHC. **a** ANT2 expression in hepatocellular carcinoma based on differentiation subtypes. **b** Differing expression of ANT2 in thyroid normal and dedifferentiated cancer tissues.

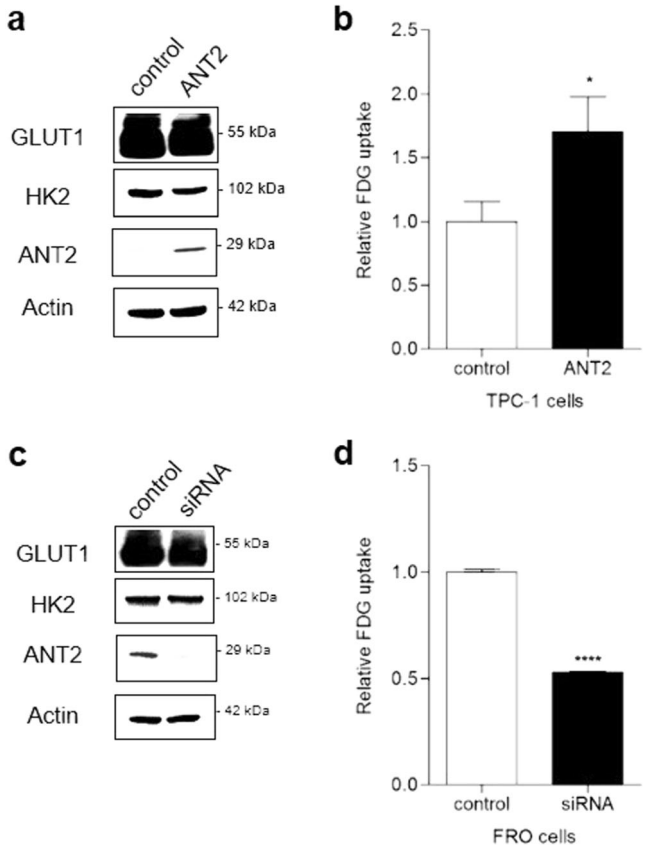

Fig. 5. Change of [18F] FDG uptake and GLUT1, HK2, and ANT2 levels after modulation of *ANT2* gene expression. **a** Changes of GLUT1, HK2, and ANT2 levels after *ANT2* upregulation in TPC-1 cells. **b** [18F] FDG uptake in ANT2-overexpressing TPC-1 cells. **c** Changes of GLUT1, HK2, and ANT2 levels after *ANT2* downregulation in FRO cells. **d** [18F] FDG uptake in FRO cells following siRNA-mediated down-regulation of *ANT2*. In both experiments, [18F] FDG uptake was correlated with ANT2 expression, regardless of the expression of GLUT1 and HK2.

[18F] FDG accumulation, and GLUT1 is a limiting factor for [18F] FDG import into the cells. Cancer cells express a large amount of HK2, which has enhanced kinase activity among the HKs. In particular, HK2 is a dimer with a dual active site that is highly expressed in rapidly proliferating cancer cells [33]. The levels of ATP, another substrate of HK2, can also be a limiting factor for cancer metabolism. In this regard, we focused on ANTs, which play a role in ATP transport and might influence [18F] FDG phosphorylation.

In human, ANTs are encoded by four homologous genes, whose expressions are dependent on the developmental stage, proliferation, and cell type [34, 35]. ANT1 is predominantly expressed in the skeletal and heart cells. ANT3 is ubiquitously expressed in somatic cells. ANT4 is exclusively expressed in germ cells, and involved in spermatogenesis [35, 36]. Among them, we focused on the ANT2 protein, which is expressed in proliferative cells, including cancer cells, and related to glycolysis [37]. The main action of ANT2 might be stabilization of mitochondria membrane permeability (MMP) and enhanced ATP production [38].

We found that [18F] FDG uptake cannot be explained by ANT2 alone. However, ANT2 could be a key factor required for [18F] FDG accumulation in various cancer cells when GLUT1 and HK2 expression are not limiting factors. Previous studies have reported that there is a relationship between the histologic features of NSCLC and [18F] FDG accumulation [39, 40]. Our data also showed that ANT2 expression was related to [18F] FDG accumulation, as well as differentiation grade and histologic types in NSCLC cells and tissues. In hepatoma, [18F]FDG-PET uptake was related to tumor differentiation, and can be used as a prognostic tool [41]; this is consistent with our results. In thyroid cancer, [18F] FDG uptake was high in poorly differentiated and anaplastic types [42–44]. Our results also suggested that ANT2 expression increased according to the dedifferentiation of thyroid cancer. Therefore, ANT2 could be regarded as a marker of dedifferentiated or more malignant type of cancer cells and tissues.

In this study, we did not compare the ANT2 expression level with therapeutic response and prognosis in cancer patients. Jang et al. [45] reported that high expression of ANT2 was related to low therapeutic response and poor prognosis in lung cancer patients treated with EGFR tyrosine kinase inhibitor (EGFR-TKI). We suggest that ANT2 expression level can be used to predict the response of targeted therapy. However, further studies are needed to clarify this point.

So far, both GLUT1 and HK2 have been reported to explain the [18F] FDG metabolism as major contributing proteins [17]. However, our results showed that ANT2 expression is involved in [18F] FDG uptake regardless of GLUT1 and HK2 expression. In this regard, we investigated the effect of modulating the ANT2 expression on [18F] FDG accumulation through *in vitro* and *in vivo* experiments. We found that the upregulation or downregulation of ANT2 expression did not affect the levels of GLUT1 and HK2, and some mitochondrial proteins such as VDAC, ANT1, and ANT3 (data was not shown), but these modulation only affected [18F] FDG accumulation. Some studies reported that the membrane potential and viability in ANT2 modulation cells were unchanged [46, 47]. Our findings were concordant with them (data was not shown). These findings suggest that ANT2 expression does not affect intracellular physiological changes, but is associated with the HK2-mediated phosphorylation process in [18F] FDG accumulation, *via* the increased provision of ATP.

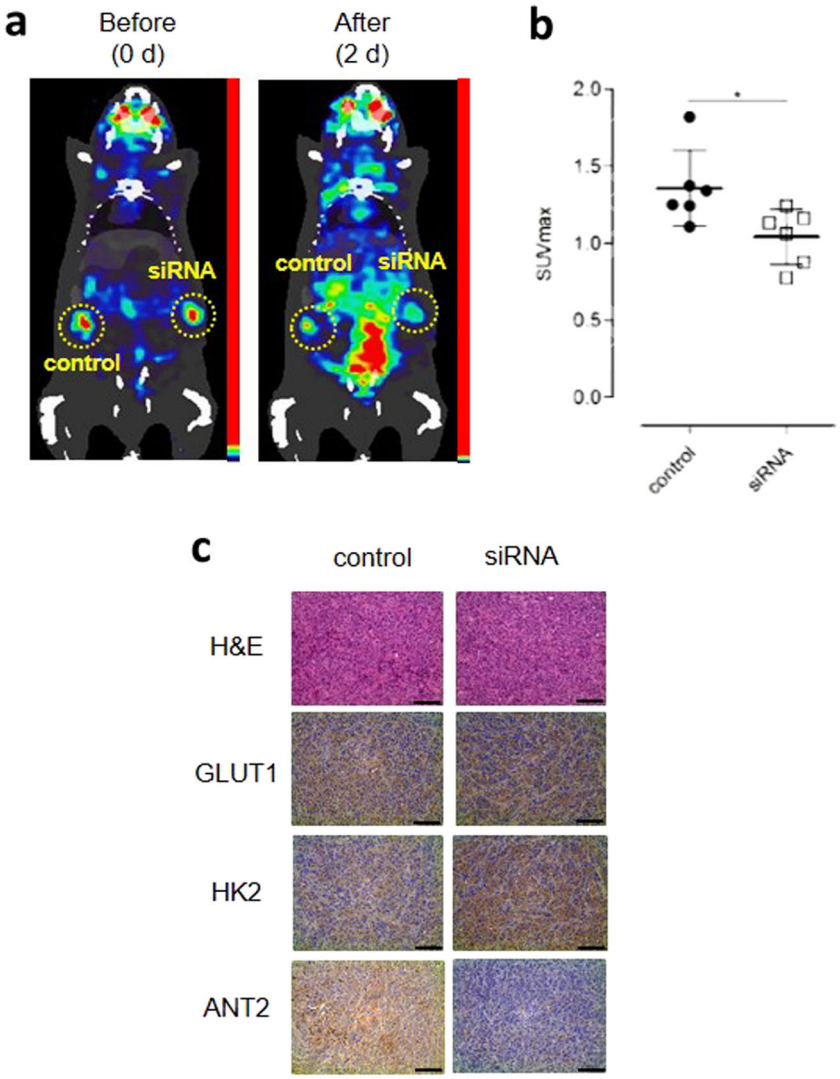

Fig. 6. Comparison between [18F]FDG-PET and IHC findings after intra-tumoral *ANT2* siRNA injection. **a** Coronal image of [18F]FDG-PET before and 48 h after ANT2 siRNA treatment. SUVmax was reduced after the siRNA treatment. **b** Tumor sections stained with GLUT1, HK2, and ANT2, as well as hematoxylin and eosin. ANT2 expression specifically decreased in tumor-treated siRNA. Scale bar 100 μm.

A limitation of this study is that we used tissue microarrays for IHC. In cases involving the heterogeneous expression of the target protein, tissue microarrays might be unsuitable, because only a few microscopic fields were evaluated. Although we found that almost all tissues showed a somewhat uniform distribution of ANT2, studies on a more number of cancer cell lines and tissues are required to confirm such relationships.

Conclusion

ANT2 expression was positively related to [18F] FDG accumulation in various cancer cells and tissues. [18F] FDG uptake was better explained by the expression levels of ANT2 than by those of GLUT1 and HK2. We modulated the expression of the *ANT2* gene and found that [18F] FDG accumulation was regulated by ANT2 expression, regardless of the levels of GLUT1 and HK2. [18F] FDG and ANT2 expression were partially related to differentiation states or the malignancy of cancer, suggesting a role of ANT2 as a marker of differentiation status and tumor aggressiveness.

Funding Information This work was supported by grants from the National Research Foundation, Ministry of Science and ICT (2011-0030001 for J-K.C. and H.Y., 2017-R1A2B4012813 for H.Y.), and the Korea Health Technology R&D Project, Ministry of Health & Welfare, Republic of Korea (HI14C1072 for K.W.K, G.J.C. and H.Y., HI15C2971 for H.Y.).

Compliance with Ethical Standards The study has been approved by the Institutional Review Board and all subjects signed an informed consent form.

Conflict of Interest

The authors declare that they have no conflict of interest.

References

1. Warburg O (1956) On the origin of cancer cells. Science 123:309–314
2. Vander Heiden MG, Cantley LC, Thompson CB (2009) Understanding the Warburg effect: the metabolic requirements of cell proliferation. Science 324:1029–1033
3. Kroemer G, Pouyssegur J (2008) Tumor cell metabolism: cancer's Achilles' heel. Cancer Cell 13:472–482
4. Kubota K, Matsuzawa T, Fujiwara T, Ito M, Hatazawa J, Ishiwata K, Iwata R, Ido T (1990) Differential diagnosis of lung tumor with positron emission tomography: a prospective study. J Nucl Med 31:1927–1932
5. Gambhir SS, Czernin J, Schwimmer J et al (2001) A tabulated summary of the FDG PET literature. J Nucl Med 42(Suppl 5):1S–93S
6. Gambhir SS (2002) Molecular imaging of cancer with positron emission tomography. Nat Rev Cancer 2:683–693
7. Pieterman RM, van Putten JW, Meuzelaar JJ et al (2000) Preoperative staging of non-small-cell lung cancer with positron-emission tomography. N Engl J Med 343:254–261
8. Antoniou AJ, Marcus C, Tahari AK, Wahl RL, Subramaniam RM (2014) Follow-up or surveillance ^{18}F-FDG PET/CT and survival outcome in lung cancer patients. J Nucl Med 55:1062–1068
9. Smith TA (1998) FDG uptake, tumour characteristics and response to therapy: a review. Nucl Med Commun 19:97–105
10. Pauwels EK, McCready VR, Stoot JH et al (1998) The mechanism of accumulation of tumor-localising radiopharmaceuticals. Eur J Nucl Med 25:277–305
11. Gallagher BM, Fowler JS, Gutterson NI, MacGregor R, Wan CN, Wolf AP (1978) Metabolic trapping as a principle of radiopharmaceutical design: some factors responsible for the biodistribution of [^{18}F] 2-deoxy-2-fluoro-D-glucose. J Nucl Med 19:1154–1161
12. Pauwels EK, Ribeiro MJ, Stoot JH et al (1998) FDG accumulation and tumor biology. Nucl Med Biol 25:317–322
13. Szablewski L (2013) Expression of glucose transporters in cancers. Biochim Biophys Acta 1835:164–169
14. Smith TA (2000) Mammalian hexokinases and their abnormal expression in cancer. Br J Biomed Sci 57:170–178
15. Hay N (2016) Reprogramming glucose metabolism in cancer: can it be exploited for cancer therapy? Nat Rev Cancer 16:635–649
16. Patra KC, Wang Q, Bhaskar PT, Miller L, Wang Z, Wheaton W, Chandel N, Laakso M, Muller WJ, Allen EL, Jha AK, Smolen GA, Clasquin MF, Robey RB, Hay N (2013) Hexokinase 2 is required for tumor initiation and maintenance and its systemic deletion is therapeutic in mouse models of cancer. Cancer Cell 24:213–228
17. Smith TA (2001) The rate-limiting step for tumor [^{18}F]fluoro-2-deoxy-D-glucose (FDG) incorporation. Nucl Med Biol 28:1–4
18. Mertens K, Mees G, Lambert B, van de Wiele C, Goethals I (2012) In vitro 2-deoxy-2-[^{18}F]fluoro-D-glucose uptake: practical considerations. Cancer Biother Radiopharm 27:183–188
19. Jadvar H, Alavi A, Gambhir SS (2009) ^{18}F-FDG uptake in lung, breast, and colon cancers: molecular biology correlates and disease characterization. J Nucl Med 50:1820–1827
20. Alvarez JV, Belka GK, Pan TC, Chen CC, Blankemeyer E, Alavi A, Karp JS, Chodosh LA (2014) Oncogene pathway activation in mammary tumors dictates FDG-PET uptake. Cancer Res 74:7583–7598
21. Riedl CC, Akhurst T, Larson S, Stanziale SF, Tuorto S, Bhargava A, Hricak H, Klimstra D, Fong Y (2007) ^{18}F-FDG PET scanning correlates with tissue markers of poor prognosis and predicts mortality for patients after liver resection for colorectal metastases. J Nucl Med 48:771–775
22. Robey RB, Hay N (2006) Mitochondrial hexokinases, novel mediators of the antiapoptotic effects of growth factors and Akt. Oncogene 25:4683–4696
23. Golshani-Hebroni SG, Bessman SP (1997) Hexokinase binding to mitochondria: a basis for proliferative energy metabolism. J Bioenerg Biomembr 29:331–338
24. Pedersen PL (2008) Voltage dependent anion channels (VDACs): a brief introduction with a focus on the outer mitochondrial compartment's roles together with hexokinase-2 in the "Warburg effect" in cancer. J Bioenerg Biomembr 40:123–126
25. Gogvadze V, Zhivotovsky B, Orrenius S (2010) The Warburg effect and mitochondrial stability in cancer cells. Mol Asp Med 31:60–74
26. Mathupala SP, Ko YH, Pedersen PL (2006) Hexokinase II: cancer's double-edged sword acting as both facilitator and gatekeeper of malignancy when bound to mitochondria. Oncogene 25:4777–4786
27. Klingenberg M (2008) The ADP and ATP transport in mitochondria and its carrier. Biochim Biophys Acta 1778:1978–2021
28. Le Bras M, Borgne-Sanchez A, Touat Z et al (2006) Chemosensitization by knockdown of adenine nucleotide translocase-2. Cancer Res 66:9143–9152
29. Chevrollier A, Loiseau D, Reynier P, Stepien G (2011) Adenine nucleotide translocase 2 is a key mitochondrial protein in cancer metabolism. Biochim Biophys Acta 1807:562–567
30. Gavaldà-Navarro A, Mampel T, Viñas O (2016) Changes in the expression of the human adenine nucleotide translocase isoforms condition cellular metabolic/proliferative status. Open Biol 6:150108
31. Perisic L, Hedin E, Razuvaev A, Lengquist M, Osterholm C, Folkersen L, Gillgren P, Paulsson-Berne G, Ponten F, Odeberg J, Hedin U (2013) Profiling of atherosclerotic lesions by gene and tissue microarrays reveals PCSK6 as a novel protease in unstable carotid atherosclerosis. Arterioscler Thromb Vasc Biol 33:2432–2443
32. Chiu YL, Rana TM (2003) siRNA function in RNAi: a chemical modification analysis. RNA 9:1034–1048
33. Mathupala SP, Ko YH, Pedersen PL (2009) Hexokinase-2 bound to mitochondria: Cancer's stygian link to the "Warburg effect" and a pivotal target for effective therapy. Semin Cancer Biol 19:17–24
34. Stepien G, Torroni A, Chung AB et al (1992) Differential expression of adenine nucleotide translocator isoforms in mammalian tissues and during muscle cell differentiation. J Biol Chem 267:14592–14597
35. Brenner C, Subramaniam K, Pertuiset C, Pervaiz S (2011) Adenine nucleotide translocase family: four isoforms for apoptosis modulation in cancer. Oncogene 30:883–895
36. Brower JV, Rodic N, Seki T, Jorgensen M, Fliess N, Yachnis AT, McCarrey JR, Oh SP, Terada N (2007) Evolutionarily conserved mammalian adenine nucleotide translocase 4 is essential for spermatogenesis. J Biol Chem 282:29658–29666
37. Chevrollier A, Loiseau D, Chabi B, Renier G, Douay O, Malthièry Y, Stepien G (2005) ANT2 isoform required for cancer cell glycolysis. J Bioenerg Biomembr 37:307–316
38. Kim HS, Je JH, Son TG, Park HR, Ji ST, Pokharel YR, Jeon HM, Kang KW, Kang HS, Chang SC, Kim HS, Chung HY, Lee J (2012) The hepatoprotective effects of adenine nucleotide translocator-2 against aging and oxidative stress. Free Radic Res 46:21–29
39. Vesselle H, Schmidt RA, Pugsley JM et al (2000) Lung cancer proliferation correlates with [F-18] fluorodeoxyglucose uptake by positron emission tomography. Clin Cancer Res 6:3837–3844
40. Vesselle H, Salskov A, Turcotte E, Wiens L, Schmidt R, Jordan CD, Vallières E, Wood DE (2008) Relationship between non-small cell lung cancer FDG uptake at PET, tumor histology, and Ki-67 proliferation index. J Thorac Oncol 3:971–978
41. Seo S, Hatano E, Higashi T, Hara T, Tada M, Tamaki N, Iwaisako K, Ikai I, Uemoto S (2007) Fluorine-18 fluorodeoxyglucose positron emission tomography predicts tumor differentiation, P-glycoprotein expression, and outcome after resection in hepatocellular carcinoma. Clin Cancer Res 13(2 Pt 1):427–433
42. Abraham T, Schöder H (2011) Thyroid cancer–indications and opportunities for positron emission tomography/computed tomography imaging. Semin Nucl Med 41:121–138
43. Bogsrud TV, Karantanis D, Nathan MA, Mullan BP, Wiseman GA, Kasperbauer JL, Reading CC, Hay ID, Lowe VJ (2008) ^{18}F-FDG PET in the management of patients with anaplastic thyroid carcinoma. Thyroid 18:713–719
44. Are C, Shaha AR (2006) Anaplastic thyroid carcinoma: biology, pathogenesis, prognostic factors, and treatment approaches. Ann Surg Oncol 13:453–464
45. Jang JY, Kim YG, Nam SJ, Keam B, Kim TM, Jeon YK, Kim CW (2016) Targeting adenine nucleotide translocase-2 (ANT2) to overcome resistance to epidermal growth factor receptor tyrosine kinase inhibitor in non-small cell lung Cancer. Mol Cancer Ther 15:1387–1396
46. Prabhu D, Goldstein AC, El-Khoury R et al (2015) ANT2-defective fibroblasts exhibit normal mitochondrial bioenergetics. Mol Genet Metab Rep 3:43–46
47. Cho J, Zhang Y, Park SY, Joseph AM, Han C, Park HJ, Kalavalapalli S, Chun SK, Morgan D, Kim JS, Someya S, Mathews CE, Lee YJ, Wohlgemuth SE, Sunny NE, Lee HY, Choi CS, Shiratsuchi T, Oh SP, Terada N (2017) Mitochondrial ATP transporter depletion protects mice against liver steatosis and insulin resistance. Nat Commun 8:14477